

Morphology, thermal, and electrical properties of polypropylene hybrid composites co-filled with multi-walled carbon nanotubes and graphene nanoplatelets

Marcin Wegrzyn,¹ Begoña Galindo,¹ Adolfo Benedito,¹ Enrique Gimenez²

¹Instituto Tecnológico del Plástico (AIMPLAS), Calle Gustave Eiffel 4, 46980 Paterna, Spain

²Instituto de Tecnología de Materiales. Universidad Politécnica de Valencia, Camino de Vera, 46022 Valencia, Spain

Correspondence to: M. Wegrzyn (E-mail: marcinwegrzyn@hotmail.com)

ABSTRACT: In this study, nanocomposites of polypropylene (PP) with various loadings of multi-wall carbon nanotubes (MWCNT) and graphene nanoplatelets (GnP) were formed by masterbatch dilution/mixing approach from individual masterbatches PP-MWCNT and PP-GnP. Melt mixing on a twin-screw extruder at two different processing temperatures was followed by characterization of morphology by transmitted-light microscopy including the statistical analysis of agglomeration behavior. The influence of processing temperature and weight fractions of both nanofillers on the dispersion quality is reported. Thermal properties of the nanocomposites investigated by DSC and TGA show sensitivity to the nanofillers weight fraction ratio and to processing conditions. Electrical conductivity is observed to increase up to an order of magnitude with the concentration of each nanofiller increasing from 0.5 wt % to 1.0 wt %. This is related with a decrease of electrical conductivity observed for unequal concentration of both nanofillers. This particular behavior shows the increase of electrical properties for higher MWCNT loadings and the increase of thermo-mechanical properties for higher GnP loadings. © 2015 Wiley Periodicals, Inc. *J. Appl. Polym. Sci.* **2015**, *132*, 42793.

KEYWORDS: extrusion; graphene and fullerenes; nanotubes; polyolefins

Received 25 January 2015; accepted 28 July 2015

DOI: 10.1002/app.42793

INTRODUCTION

Carbon nanotubes have gained the attention of material science community confirming the ability to boost electrical and thermal properties of insulating polymers.^{1,2} Uncommon properties of this material being a result of a unique structure and a high aspect ratio enable an improvement of mechanical properties of polymer matrices.^{3,4} However, carbon nanotubes often described as one-dimensional structures are recently confronted with the two-dimensional graphene, when polymer filling is in consideration.⁵ Even though the aim of formation the graphene oxide-based nanocomposites is usually an increase of mechanical properties,⁶ a significant influence on electrical and thermal properties has been reported in these materials.⁷ The main issue that distracts the desired improvement of polymers is the reported for both nanomaterials difficulty in achieving homogeneous dispersions in thermoplastic matrix.^{8,9} The agglomeration behavior of individual nanoparticles is driven by the attractive Van der Waals forces between the individual nanoparticles and can be reduced in extrusion process by a proper selection of processing conditions.¹⁰ This is related with a breakage of primary carbon nanotube agglomerates in the process of

macrostructure penetration by polymer melt¹⁰ or by the exfoliation of graphite to obtain monolayer sheets of graphene nanoplatelets.¹¹ Usually proper processing parameters including high screw speed and low barrel temperature provide homogeneous morphologies. However, these conditions must be included in the specific mechanical energy (SME) defining the energy applied to the nanocomposite melt during melt-mixing.¹² Mutual relation between viscosity of thermoplastic melt, screw speed, and temperature profile applied during processing is a complex phenomenon. Thus, the use of SME is usually suggested to have a proper control over the entire nanocomposite system.

The examples of melt-mixed nanocomposites with matrices of commodity polymers exist in the literature with carbon-based fillers, carbon nanotubes or graphene nanoplatelets: polyethylene (PE),^{13,14} polypropylene (PP),^{15,16} and polystyrene (PS).^{17,18} Nevertheless, polymer-based nanocomposites co-filled with these nanofillers in order to form a hybrid system are studied mainly with scientific approach.^{19,20} Reports show the tendency of quite common use of thermoset matrix for such study of complex filler systems.^{21,22} On the basis of these works, the synergistic

Table I. Nanofillers Content in Prepared Nanocomposites and Samples Codification

Sample code	MWCNT content	GnP content	Total nanofiller content
0.5T/0.5P	0.5 wt %	0.5 wt %	1.0 wt %
0.5T/1.0P	0.5 wt %	1.0 wt %	1.5 wt %
1.0T/0.5P	1.0 wt %	0.5 wt %	1.5 wt %
1.0T/1.0P	1.0 wt %	1.0 wt %	2.0 wt %

effect and carbon nanotubes-to-graphene nanoplatelets ratio are shown to influence the key final properties, for example, tensile strength. Furthermore, alignment of carbon nanotubes or graphene flakes caused by the shear during processing causes the formation of an interconnected network in the matrix²¹ giving a significant improvement of thermal conductivity.²² To obtain better dispersions of nanophase and boost the final properties, the additives like wax²³ or surfactants²⁴ are commonly used in the preparation process of nanocomposites with thermoplastic matrix. Thus, an increase of electrical and mechanical properties in thermoplastic nanocomposites co-filled with MWCNT and GnP is correlated with the morphology. This is observed for both: semi-crystalline^{23,25} and amorphous²⁴ matrices. Besides that, semi-crystalline polymers show an increase of crystallinity after the incorporation of carbon nanotubes or graphene nanoplatelets, which is explained by the nucleation effects.²⁵

In this study, we present PP-MWCNT/GnP nanocomposites prepared with scalable industrial approach by mixing and dilution of pre-dispersed masterbatches on twin-screw extruder at two processing temperatures. These multi-phase nanocomposites may be used in electronic or electric industries replacing mono-filled nanocomposites and providing wider range of improved properties (e.g., increase of electrical conductivity and decrease of flammability). Such an attempt of nanocomposites preparation is usually omitted in the field of co-filled thermoplastics research and this study is an initial attempt, which will eventually lead to deeper understanding of this area. Various nanofillers content and control of nanofillers ratio allowed studying the influence of synergy effects. The effects of specific mechanical energy (SME) applied to the material during processing shows the influence of used temperature profiles. Morphology of the nanocomposites is characterized by the light-transmission microscopy (LTM) and agglomeration behavior is determined by statistical methods. Thermal properties investigated by thermo-gravimetric analyses (TGA) and differential scanning calorimetry (DSC) along with thermo-mechanical properties studied by dynamic-mechanical analysis (DMA) show relationship with the morphology.

EXPERIMENTAL

Materials

Commercial polypropylene (PP) Domolen 1101S (MFR 24 g/10 min) was supplied by DOMO Chemicals. Multi-walled carbon nanotubes (MWCNT) NC7000 with average diameter 9.5 nm, average length 1.5 μm , and surface area ranging between 250 and 300 m^2/g were supplied by Nanocyl (95% purity).

Graphene nanoplatelets (GnP) xGnP-M5 with average thickness 5–8 nm, average particle diameter 5 μm , and surface area ranging between 120 and 150 m^2/g were supplied by XG Sciences (over 98% purity). Graphene nanoplatelets were used as received, without any modifications.

Preparation of Nanocomposites

Nanocomposites with various nanofillers concentration (Table I) were prepared with masterbatch mixing/dilution approach. Masterbatches of polypropylene/multi-walled carbon nanotubes (PP-MWCNT) and polypropylene/graphene nanoplatelets (PP-GnP) (each containing 15 wt. % nanofiller) were prepared by melt-mixing on a Coperion ZSK 25 co-rotating twin-screw extruder with a screw speed 600 rpm, barrels temperature 170–200°C and a throughput 6 kg/h. The final nanocomposites were subsequently formed by mixing the PP-MWCNT and the PP-GnP masterbatches with neat polypropylene at various ratios to concentrations present in Table I. The formation of final nanocomposites was carried out on a Prism Eurolab 16 (Thermo Fisher Scientific) co-rotating twin-screw extruder (L/D 25). Nanocomposites were produced at two screw temperature profiles: 170–200°C (low temperature profile) or 190–240°C (high temperature profile) with a screw speed 600 rpm.

Rectangular samples with dimensions 60 x 10 x 2 mm^3 (following the modified standard ISO 127) were compression-molded on a Collin 6300 hydraulic press at 190°C. A 20-minute five-step program was applied in order to produce specimens that can be used in electrical conductivity measurements. Slow cooling with air was applied to all produced specimens in order to reduce structural stresses.

Characterization

Morphology of the nanocomposites studied by transmitted-light microscopy (LTM) on a Leica DMRX microscope. Films (thickness 20–50 μm) used in this experiment were hot-pressed from pellets. Experiments were repeated on three representative samples for each material and the values given here are average values. Agglomeration behavior, including agglomeration density, was studied via Leica Materials Workstation software. Agglomerates in this software were determined on high-contrast images as dark regions on a bright background. The agglomeration density was evaluated as a ratio of agglomerated area to the total investigated area of measured discs.

Thermo-gravimetric analysis (TGA) was done on a Q5000 instrument (TA Instruments). Pellets weighting 10 mg were heated from 50°C to 800°C at a heating rate of 20°C/min in nitrogen atmosphere. Differential scanning calorimetry (DSC) was done on a Diamond (Perkin-Elmer). Each sample was heated from 40°C to 240°C at a heating rate of 10°C/min to erase the thermal history. This was followed by cooling to 40 °C at the same rate and then by a second heating to 240°C to determine the melting points and enthalpies. Dynamic-mechanical analyses (DMA) was done on a TA Instrument DMA-2980 with dual cantilever clamp at a vibration frequency 1 Hz, between 35°C and 200°C at scan rate 3°C/min. Experiments were repeated three times for each material.

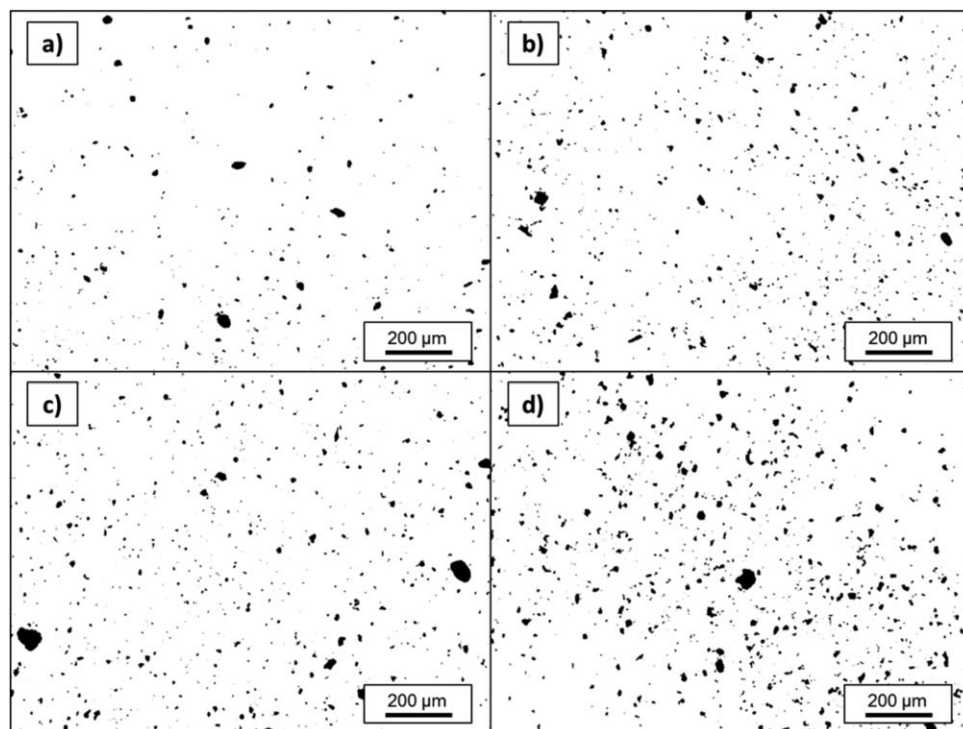


Figure 1. Light-transmission microscopy of polypropylene nanocomposites: (a) 0.5T/0.5P Low temperature profile, (b) 1.0T/1.0P Low temperature profile, (c) 0.5T/0.5P High temperature profile, (d) 1.0T/1.0P High temperature profile.

Electrical resistivity was measured by two-point contact configuration (following the ISO 3915 standard) on a Keithley 2000 Multimeter source/meter. Silver electrodes were painted on the samples in order to improve contact with the measuring electrodes.

RESULTS AND DISCUSSION

Macro-scale morphology of nanocomposites obtained by dilution of a pellets mixture containing PP-MWCNT and PP-GnP with the virgin PP is shown on the LTM images in Figures 1 and 2. The nanofillers dispersion level achieved for the studied MWCNT-GnP contents and for both temperature profiles applied during the dilution step varies. The study of these differences is divided between the fillers weight fraction ratio equal 1.0 (representing the same share of both fillers in the nanocomposite, shown in Figure 1) and unequal 1.0 (representing different shares of each filler in the total loading, shown in Figure 2). Thus, an increase of agglomeration behavior is observed for higher nanofillers loading at both processing conditions shown in Figure 1. Furthermore, a clearly higher number of agglomerates is observed at high temperature profile for both compositions: 0.5T/0.5P (Figure 1c) and 1.0T/1.0P (Figure 1d). This effect can be explained by an expected decrease of matrix viscosity at higher processing temperatures, causing a reduction of force necessary for agglomerates breakage.

However, an uneven fillers weight fraction brings a deviation from this observation decreasing the nanocomposites sensitivity to processing conditions. No significant changes in agglomeration behavior are observed between 0.5T/1.0P processed at low temperature profile [Figure 2(a)] and at high temperature pro-

file (Figure 2c). Analogous observation can be made for an opposite ratio of nanofillers loadings: 1.0T/0.5P [Figure 2(b,d)]. Nevertheless, a clear decrease of agglomerates number occurs when a nanocomposite contains higher loadings of multi-walled carbon nanotubes than graphene nanoplatelets. Such a change of morphology at similar total loadings of nanofillers is observed for both applied processing conditions. This can be explained by various MWCNT and GnP dispersion abilities in PP matrix and by interfacial forces between both nanomaterials or between each nanofiller and the matrix. Besides, graphene is known for its lubricating properties, which can cause an unwanted effect of the reduction of exfoliation/agglomerate breakage efficiency.²⁶ The presence of graphene may reduce interlaminar binding and cause slipping, which significantly reduces the final dispersion quality. On the other hand, carbon nanotubes are known to give uniform nanocomposites in different polymer matrices, which explain more homogeneous morphology of 1.0T/0.5P [e.g., Figure 2(a)] than 0.5T/1.0P [e.g., Figure 2(b)]. Nevertheless, nanofiller dispersions in a mono-filled MWCNT-based nanocomposites are not subjected to the negative aforementioned influence of lubricant reducing interfacial forces between polypropylene and MWCNT, which reduces shear during melt-mixing. Thus, theoretically these nanocomposites should give more homogeneous morphologies than the co-filled materials studied in this work.

Agglomeration behavior directly influencing the final morphology of PP-MWCNT/GnP nanocomposites is related with the specific mechanical energy (SME). Curves shown in the graph in Figure 3 are calculated with Equation (1), which includes εP representing effective power of the motor, τ representing torque,

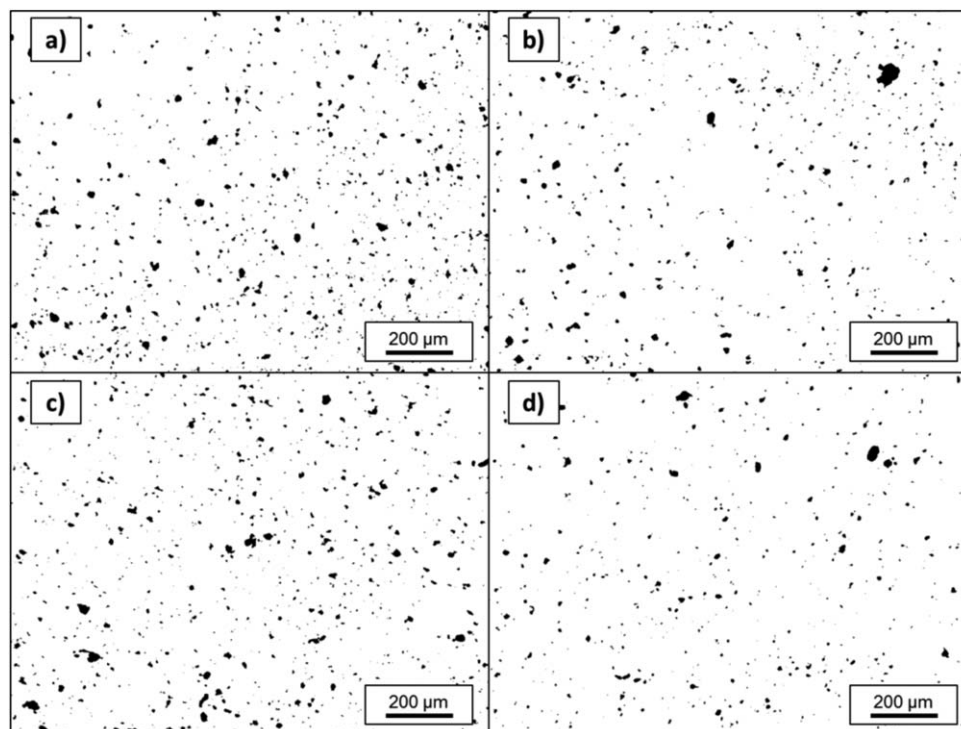


Figure 2. Light-transmission microscopy of polypropylene nanocomposites: (a) 0.5T/1.0P Low temperature profile, (b) 1.0T/0.5P Low temperature profile, (c) 0.5T/1.0P High temperature profile, (d) 1.0T/0.5P High temperature profile.

and v_{proc}/v_{max} – screw speeds ratio. The throughput Q was constant in the studied experiments. However, the influence of this parameter is reported in the literature.¹²

$$SME = \frac{\varepsilon P \cdot \tau \cdot \frac{v_{proc}}{v_{max}}}{Q} \quad (1)$$

Therefore, the SME values for different nanofillers weight fractions shows how effective the processing conditions are for a specific composition. The energy applied to the material during the masterbatches dilution step varies significantly between applied temperature profiles. Lower processing temperature provides higher energy due to a higher viscosity of the melt. This is confirmed by the morphological study, where nanocomposites of the same compositions give better dispersions at low temper-

ature profile [Figure 1(a,c)]. Besides that, an expected increase of SME is observed between 0.5T/0.5P and 1.0T/1.0P that is also related with increase of melt viscosity coming from the nanomaterials network formation in the polymer melt. Furthermore, the higher values of specific mechanical energy are observed for the compositions with higher carbon nanotube concentration (1.0T/0.5P), which is also related with the formation of continuous, interconnected network in polymer melt affecting the rheology of the whole system. The one-dimensional structures (MWCNT) are capable of forming such networks at significantly lower weight fractions than the flake-like structures (GnP) and this is the explanation why the hybrid nanofillers system with higher carbon nanotubes loading give higher torque readings than the analogous system with the increased graphene nanoplatelets concentration. The aforementioned difference between morphology of 1.0T/0.5G [Figure 2(d)] and 0.5T/1.0P [Figure 2(c)], showing higher homogeneity of the former nanocomposite, confirms the conclusions of SME behavior.

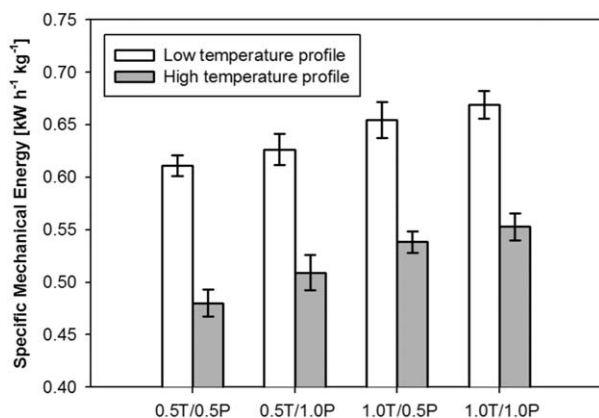


Figure 3. Specific mechanical energy of polypropylene nanocomposites at different processing conditions.

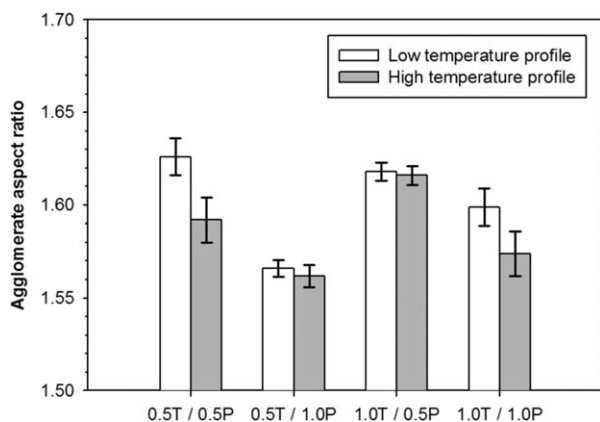
The quality of nanocomposites morphology is additionally studied with the statistical methods based on agglomeration behavior investigated on LTM images. Tables II and III contain the parameters description of the agglomeration behavior of PP-MWCNT/GnP nanocomposites. Agglomerate length and agglomerate area (Table II) for the nanocomposites with fillers concentration ratio 1 : 1 (0.5T/0.5P and 1.0T/1.0P) show similar increase pattern with the nanofiller weight fraction for both studied temperature profiles. Such an effect is already described in the discussion of transmitted-light microscopy test (Figure 1). The influence of processing showing the decreasing

Table II. Agglomerate Length and Agglomerate Area in Polypropylene Nanocomposites Filled with Carbon Nanotubes and Graphene Nanoplatelets

	Agglomerate length [μm]		Agglomerate Area [μm^2]	
	Low temp. profile	High temp. profile	Low temp. profile	High temp. profile
0.5T/0.5P	9.794 (\pm 0.17)	10.210 (\pm 0.09)	55.628 (\pm 2.06)	61.163 (\pm 1.51)
0.5T/1.0P	10.761 (\pm 0.30)	10.872 (\pm 0.11)	66.747 (\pm 0.97)	71.106 (\pm 3.02)
1.0T/0.5P	10.056 (\pm 0.25)	10.359 (\pm 0.16)	58.964 (\pm 3.21)	66.232 (\pm 4.28)
1.0T/1.0P	10.697 (\pm 0.42)	12.002 (\pm 0.21)	69.477 (\pm 4.17)	86.209 (\pm 5.10)

agglomeration behavior when the low temperature profile is applied also agrees with the previous findings of the improved morphology for materials formed at such conditions. Besides that, the higher average values of agglomerate area and agglomerate length for 0.5T/1.0P than for 1.0T/0.5P correspond with the LTM images showing more homogeneous morphology for the latter nanocomposites (Figure 2). However, Figure 4 presenting the aspect ratio of individual agglomerates at applied conditions shows the trend opposite to the one observed in Table I. Analysis of this parameter suggests that the agglomerate shape is more spherical at elevated nanofiller loadings, at high processing temperature and when the sample contains higher content of GnP than MWCNT. All mentioned factors show also the negative effect on morphology. Thus the agglomerate aspect ratio should be directly related to the shear forces occurring in a twin-screw extruder and to the viscosity of the nanocomposite melt. Furthermore, the presence of co-nanofiller most probably distracts the whole system. Thus, the morphology of nanocomposite that is theoretically possible when each of the used nanofillers is individually dispersed in polypropylene will show worse performance for the hybrid-filler system.

A parameter shown in Table III represents the agglomerate size distribution and is defined as the largest agglomerate size within the 95% of the smallest agglomerates observed in the specimen. An expected increase of this value for the increase of MWCNT/GnP content from 0.5T/0.5P to 1.0T/1.0P is observed. Besides that, the aforementioned in Figure 1 pattern of higher agglomeration presence in nanocomposites processed at high temperature profile agrees with the data in Table III. Regarding the 95%

**Figure 4.** Agglomerate aspect ratio in polypropylene nanocomposites extruded at various temperature profiles.

population parameter for materials with uneven concentrations of MWCNT and GnP, the 0.5T/1.0P with characteristic poor morphology (when compared to the corresponding 1.0T/0.5P) shows high values. This is understood as a wider agglomerate size distribution and can be noticed in LTM images in Figure 2(a).

Thermal properties of PP nanocomposites co-filled with carbon nanotubes and graphene nanoplatelets were studied on data collected during the DSC experiment. Table IV shows the linear decrease of melting point onset and melting enthalpy (ΔH) with a gradual increase of nanofillers weight fraction. Similar behavior of melting temperature observed on other thermoplastic nanocomposites with the plate-like particles is reported to indicate a reduced degree of crystallinity at higher contents.²⁷ Crystallinity in PP-MWCNT/GnP varied between 28% (polypropylene) and 37% decreasing with the same pattern. There is no significant difference greater than, c.a., 5% between the two applied temperature profiles. However, the values are slightly higher for low nanofiller loadings and at low temperature profile. This is an indirect indication of the quality of material morphology, since the nano-size fillers act in semi-crystalline matrices as nucleating agents. Furthermore, unexpectedly within the uneven filler ratio materials the crystallinity values are higher for the compositions with less carbon nanotubes. This can be related to the possible superior PE nucleation properties of graphene nanoplatelets. It is believed that interactions (e.g. hydrogen bonds) between graphene and polymer chains are initiating further similar bonds between chains, causing crystallite growth. Besides, the well-dispersed nanofiller forming a network in the matrix usually cause an increase of transition temperatures.²⁸ Reduced confinement of polymer chains in the presence of agglomerated MWCNT and GnP restricts the formation of perfect crystals. Therefore, a high nanofillers content of 1.0T/1.0P and the presence of agglomerates distract the crystallites

Table III. Agglomerates Distribution in Polypropylene Nanocomposites Filled with Carbon Nanotubes and Graphene Nanoplatelets

	95% population [μm]	
	Low temp. profile	High temp. profile
0.5T/0.5P	20.0 (\pm 0.35)	20.5 (\pm 0.20)
0.5T/1.0P	21.5 (\pm 0.39)	22.0 (\pm 0.28)
1.0T/0.5P	20.0 (\pm 0.48)	21.5 (\pm 0.43)
1.0T/1.0P	22.0 (\pm 0.51)	24.0 (\pm 0.62)

Table IV. Melting Temperature of Polypropylene Nanocomposites Filled with Carbon Nanotubes and Graphene Nanoplatelets

	Peak onset [°C]		ΔH [J/g]	
	Low temp. profile	High temp. profile	Low temp. profile	High temp. profile
PP	155.79 (\pm 0.09)	155.92 (\pm 0.09)	108.92 (\pm 0.11)	108.76 (\pm 0.10)
0.5T/0.5P	153.42 (\pm 0.75)	153.59 (\pm 0.83)	106.85 (\pm 0.36)	107.64 (\pm 0.34)
0.5T/1.0P	149.87 (\pm 0.65)	150.93 (\pm 0.10)	106.06 (\pm 0.16)	106.57 (\pm 0.27)
1.0T/0.5P	150.98 (\pm 0.64)	152.02 (\pm 0.46)	106.39 (\pm 0.14)	107.43 (\pm 0.18)
1.0T/1.0P	149.60 (\pm 0.13)	150.19 (\pm 0.05)	105.42 (\pm 0.22)	106.39 (\pm 0.33)

quality affecting the phase transition. This gives a significant reduction of melting temperature up to 3.8%. Furthermore, nanocomposites with uneven concentration of fillers give the reduced values of both investigated parameters for 0.5T/1.0P. This agrees with the LTM observations of better morphology for the material with higher content of carbon nanotubes [Figure 2(b)].

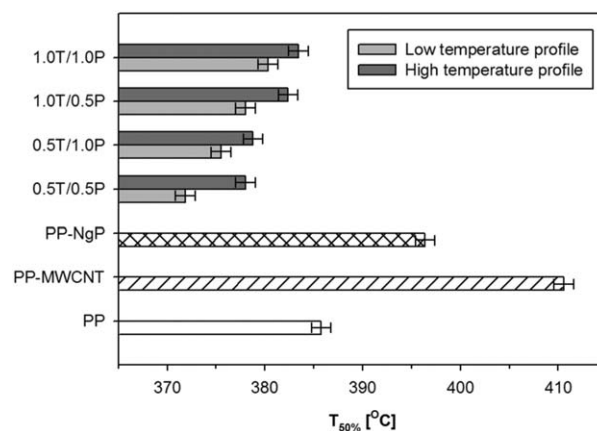
The representative results of thermo-gravimetric analysis present in Figure 5 include a half-mass loss temperature ($T_{50\%}$) observed during the thermal degradation experiment. A clear increase of matrix thermal stability for PP-MWCNT and PP-GnP nanocomposites is observed. The effect is stronger when carbon nanotubes are used as filler most probably due to the better dispersion achieved at the same processing conditions. Theoretically, these results should show a 2D material to give better results due to better barrier properties distracting the emission of combustion gases from the specimen bulk. Nevertheless, the well-dispersed carbon nanotubes form a uniform network in the matrix showing the aforementioned barrier properties at sufficient level. Besides, the formation of char on the surface of the specimen during the decomposition shows similar barrier effect. Such structure may be tighter when the nanomaterials are better distributed. Besides that, there is no synergy for the co-filled nanocomposites and a reduction of thermal stability for all PP-MWCNT/GnP materials is observed. This is most probably related with the non-sufficient homogeneity of nanofillers and the effect of morphology decrease with

the formation of hybrid system. A slight increase of $T_{50\%}$ with the increase of the total nanofiller loading is observed to be stronger when a high temperature profile is used. This suggests a major importance of the nanofiller content over the dispersion quality in thermal stability of hybrid filler system-based nanocomposites.

Thermo-mechanical properties of PP-MWCNT/GnP nanocomposites, slightly lower at low-temperature profile, are shown in Figure 6. This minimal decrease of storage modulus when lower processing temperature is applied can be explained by the matrix crystallisation behavior. However, it is believed that the crystallisation-storage modulus in case of polypropylene is only the indication of the decrease of matrix-filler interactions.²⁹ The curves of storage modulus change with the temperature do not increase linearly with the total nanofiller loading. Instead of that, the increase of storage modulus is generally observed with the increase of GnP weight fraction share in the total nanofiller loading (increase of the ratio graphene nanoplatelets-to-carbon nanotubes loading). Only material with the lowest loading (0.5T/0.5G) does not fit to this pattern, which can be explained by the insufficient total loading. The main effect is partially related with the total loading of nanofillers in polypropylene, but the composition of the co-nanofillers also seems to play an important role, which is explained by morphology and synergy effect. This can be observed by the higher value of storage modulus for 0.5T/1.0G (total nanofillers loading 1.5 wt %) than for 1.0T/1.0G (total loading 2.0 wt %). Explanation of the

Table V. Electrical Conductivity of Polypropylene Nanocomposites Filled with Carbon Nanotubes and Graphene Nanoplatelets

	Electrical conductivity [S/cm]	
	Low temp. profile	High temp. profile
0.5T/0.5P	$3.69 \cdot 10^{-4}$ (\pm $4.06 \cdot 10^{-5}$)	$4.11 \cdot 10^{-4}$ (\pm $4.94 \cdot 10^{-5}$)
0.5T/1.0P	$3.77 \cdot 10^{-6}$ (\pm $3.92 \cdot 10^{-5}$)	$8.37 \cdot 10^{-5}$ (\pm $4.31 \cdot 10^{-5}$)
1.0T/0.5P	$2.55 \cdot 10^{-5}$ (\pm $3.21 \cdot 10^{-5}$)	$1.37 \cdot 10^{-4}$ (\pm $5.14 \cdot 10^{-5}$)
1.0T/1.0P	$7.14 \cdot 10^{-4}$ (\pm $5.87 \cdot 10^{-5}$)	$1.20 \cdot 10^{-3}$ (\pm $6.02 \cdot 10^{-5}$)

**Figure 5.** Temperature of 50% weight loss of polypropylene nanocomposites extruded at various temperature profiles.

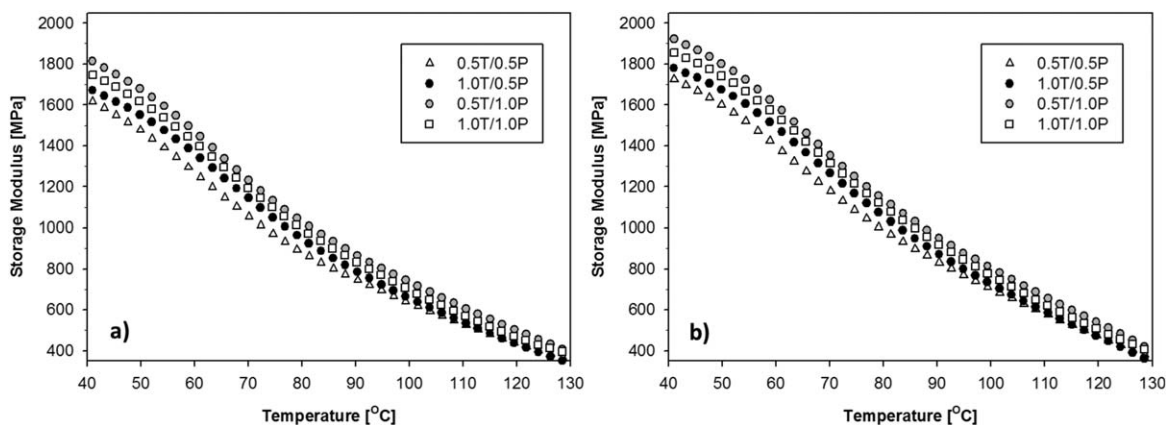


Figure 6. Storage modulus of PP/MWCNT/GnP nanocomposites extruded at various temperature profiles.

uncommon pattern in storage modulus dependence on nanofiller loading is related to the character of nanoparticles. Graphene nanoplatelets are reported to improve mechanical properties better than carbon nanotubes due to their geometry.²¹ Thus, the processing conditions seem to have comparable significance in controlling the effect of carbon-based nanofillers on thermo-mechanical properties than the loading.

Table V presents the electrical conductivity values measured by a two-point method described elsewhere.³⁰ For the nanocomposites with fillers ratio 1 : 1, a 190–200% increase of electrical conductivity is achieved with an increase of nanofiller content from 0.5 wt % (0.5T/0.5P) to 1.0 wt % (1.0T/1.0P). Such an improvement of electrical properties can be correlated with the presence of two different geometry nanofillers and with the possible presence of interconnected network of carbon nanotubes and graphene nanoplatelets. Nevertheless, a significant reduction of electrical conductivity is observed when the 1 : 1 ratio between nanofiller content is disturbed. This can be caused by a statistical need of the presence of both fillers in order to provide efficient MWCNT-GnP bridging. However, it seems that mainly one-dimensional carbon nanotubes are responsible for the electrical charge paths formation inside the matrix, which is confirmed by a c.a. 55% higher electrical conductivity of 1.0T/0.5P than 0.5T/1.0P. The presence of a good distribution and interconnection of agglomerates rather than a perfect carbon nanotube network is needed for high electrical conductivity.³¹ On the contrary, the greater improvement of electrical properties present in materials melt-mixed at higher temperature does not seem to show strong correlation with homogeneous nanofillers dispersion, which is achieved at low temperature profile (Figure 1). Thus, a high processing temperature most probably induces changes in matrix-nanofiller interactions causing an increase of conductivity. Similar effect of processing temperature was reported in thermoplastic nanocomposites.^{32,33}

CONCLUSIONS

In this study we present industrially favored approach for preparation of polypropylene nanocomposites co-filled with carbon nanotubes and graphene nanoplatelets. Masterbatches dilution/mixing approach carried out on a twin-screw extruder at two different temperature profiles shows differences in morphology

of the final nanocomposites. A clear reduction of agglomeration is observed in transmitted-light microscopy images when the nanocomposite contains higher loading of carbon nanotubes than graphene nanoplatelets. This effect is correlated with the specific mechanical energy and confirmed by a statistical study of agglomeration behavior. Furthermore, a decrease of agglomeration behavior is observed at lower applied processing temperature. A reduction of the nanocomposites melting temperature, greater for uneven nanofillers content, is explained by a distraction of matrix crystallization caused by agglomeration. Similar behavior for uneven nanofillers content is observed for electrical conductivity showing the greater decrease of values when the graphene nanoplatelets loading is higher than carbon nanotubes loading. On the contrary, the thermo-mechanical properties are improved for higher graphene content.

Electron microscopy study of nano-scale morphology in the PP-MWCNT/GnP nanocomposites needs to be performed. Besides, a more complete study of electrical conductivity in co-filled polypropylene need to be carried out in order to provide more precise data regarding the influence of processing conditions and reveal the characteristic parameters of each nanocomposite material, e.g. electrical percolation threshold.

ACKNOWLEDGMENTS

This study is funded by the European Community's Seventh Framework Program (FP7-PEOPLE-ITN-2008) within the CONTACT project Marie Curie Fellowship under grant number 238363.

REFERENCES

1. Yang, L.; Liu, F.; Xia, H.; Qian, X.; Shen, K.; Zhang, J. *Carbon* **2011**, *49*, 3274.
2. Singh, I. V.; Tanaka, M.; Endo, M. *Int. J. Therm. Sci.* **2007**, *46*, 842.
3. Kuan, H.-C.; Ma, C.-C. M.; Chang, W.-P.; Yuen, S.-M.; Wu, H.-H.; Lee, T.-M. *Compos. Sci. Technol.* **2005**, *65*, 1703.
4. Arasteh, R.; Omid, M.; Rousta, A. H. A.; Kazerooni, H. *J. Macromol. Sci. B* **2011**, *50*, 2464.

5. Martin-Gallego, M.; Verdejo, R.; Khayet, M.; Ortiz de Zarate, J. M.; Essalhi, M.; Lopez-Manchado, M. A. *Nanoscale Res. Lett.* **2011**, *610*, 1.
6. Cai, D.; Jin, J.; Yusoh, K.; Rafiq, R.; Song, M. *Compos. Sci. Technol.* **2012**, *72*, 702.
7. Yan, D.; Zhang, H.-B.; Jia, Y.; Hu, J.; Qi, X.-Y.; Zhang, Z.; Yu, Z.-Z. *ACS Appl. Mater. Interfaces* **2012**, *4*, 4740.
8. Haslam, M. D.; Raeymaekers, B. *Compos. B* **2013**, *55*, 16.
9. Kuilla, T.; Bhadra, S.; Yao, D.; Kim, N. H.; Bose, S.; Lee, J. H. *Prog. Polym. Sci.* **2010**, *35*, 1350.
10. Pötschke, P.; Dudkin, S. M.; Alig, I. *Polymer* **2003**, *44*, 5023.
11. Stankovich, S.; Dikin, D. A.; Dommett, G. H.; Kohlhaas, K. M.; Zimney, E. J.; Stach, E. A.; Piner, R. D.; Nguyen, S. T.; Ruoff, R. S. Graphene-based composite materials, *Nature* **2006**, *442*, 282.
12. Sathyanarayana, S.; Olowojoba, G.; Weiss, P.; Calgar, B.; Pataki, B.; Mikonsaari, I.; Huebner, C.; Hening, F. *Macromol. Mater. Eng.* **2013**, *298*, 89.
13. Vega, J. F.; Martinez-Salazar, J.; Trujillo, M.; Arnal, M. L.; Müller, A. J.; Bredeau, S.; Dubois, Ph. *Macromolecules* **2009**, *42*, 4719.
14. Kim, H.; Kobayashi, S.; AbdurRahim, M. A.; Zhang, M. J.; Khusainova, A.; Hillmyer, M. A.; Abdala, A. A.; Macosko, C. W. *Polymer* **2011**, *52*, 1837.
15. Alig, I.; Lellinger, D.; Dudkin, S.; Pötschke, P. *Polymer* **2007**, *49*, 1020.
16. Chaharmahali, M.; Hamzeh, Y.; Ebrahimi, G.; Ashori, A.; Ghasemi, I. *Polym. Bull.* **2014**, *71*, 337.
17. Hill, D. E.; Lin, Y.; Rao, A. M.; Allard, L. F.; Sun, Y. P. *Macromolecules* **2002**, *35*, 9466.
18. Yu, Y.-H.; Lin, Y.-Y.; Lin, C.-H.; Chan, C.-C.; Huang, Y.-C. *Polym. Chem.* **2014**, *5*, 535.
19. Zhang, S.; Yin, S.; Rong, C.; Huo, P.; Jiang, Z.; Wang, G. *Eur. Polym. J.* **2013**, *49*, 3125.
20. Huang, G.; Wang, S.; Song, P.; Wu, C.; Chen, S.; Wang, X. *Compos. A* **2014**, *59*, 18.
21. Chatterjee, S.; Nafezarefi, F.; Tai, N. H.; Schlagenhauf, L.; Nüesch, F. A.; Chu, B. T. T. *Carbon* **2012**, *50*, 5380.
22. Im, H.; Kim, J. *Carbon* **2012**, *50*, 5429.
23. Jiang, X.; Drzal, L. T. *Compos. A* **2011**, *42*, 1840.
24. Hwang, S.-H.; Park, H. W.; Park, Y.-B.; Um, M.-K.; Byun, J.-H.; Kwon, S. *Compos. Sci. Technol.* **2013**, *89*, 1.
25. Chatterjee, S.; Nüesch, F. A.; Chu, B. T. T. *Chem. Phys. Lett.* **2013**, *557*, 92.
26. Lahiri, D.; Hec, F.; Thiesse, M.; Durygin, A.; Zhang, C.; Agarwal, A. *Tribol. Int.* **2014**, *70*, 165.
27. Pavlidou, S.; Papaspyrides, C. D. *Prog. Polym. Sci.* **2008**, *33*, 1119.
28. Su, S. P.; Xu, Y. H.; Wilkie, C. A. In *Polymer-Carbon Nanotube Composites: Preparation, Properties and Applications* McNally, T.; Pötschke, P., Eds.; Woodhead Publishing: Cambridge, **2011**; Vol. 1, Chapter 16, pp 482–509.
29. Okamoto, M. In *Polymer/Layered Silicate Nanocomposites*; Humphreys, S., Ed.; Smithers Rapra Press: Shawbury, **2003**; Vol. 1, Chapter 6, pp 29–42.
30. Wegrzyn, M.; Juan, S.; Benedito, A.; Gimenez, E. *J. Appl. Polym. Sci.* **2013**, *130*, 2152.
31. Pegel, S.; Villmow, T.; Pötschke, P. In *Polymer-Carbon Nanotube Composites: Preparation, Properties and Applications*; McNally, T.; Pötschke, P., Eds.; Woodhead Publishing: Cambridge, **2011**; Vol. 1, Chapter 9, pp 265–293.
32. Zhang, R.; Moon, K.-S.; Lin, W.; Wong, C. P. *J. Mater. Chem.* **2010**, *20*, 2018.
33. Grossiord, N.; Kivitt, P. J. J.; Loos, J.; Meuldijk, J.; Kytlyuk, A. V.; van der Schoot, P.; Koning, C. E. *Polymer* **2008**, *49*, 2866.